MD simulations of the cluster beam deposition of porous Ge

A. Harjunmaa[1,a], J. Tarus[2], K. Nordlund[1], and J. Keinonen[1]

[1] Accelerator Laboratory, University of Helsinki, Finland
[2] CSC – Scientific Computing Ltd., Espoo, Finland

Abstract. The low-energy cluster beam deposition of Ge clusters on a Si surface was simulated using classical molecular dynamics. In an effort to find a suitable energy range to construct porous Ge films, the porosity of the resulting layers was mapped as a function of deposition energy. It was discovered that the energies of interest to produce porosities in the range of 30% to 70% were between about 10 meV and 500 meV per atom. Also, it became clear that the number of deposited clusters must be above 40 for the calculated porosities to be accurate. In addition, transmission electron microscope image simulations were performed on the deposited samples, and images of porous and non-porous layers were found to be distinctly different.

PACS. 68.37.Lp Transmission electron microscopy (TEM) – 81.05.Rm Porous materials

1 Introduction

The discovery of the strong visible photoluminescence of porous silicon (PS) at room temperature by Canham in 1990 [1] sparked widespread interest in the fabrication and use of porous semiconductor materials in research and industry. In addition to silicon, other porous semiconductor surfaces such as germanium [2], $Si_{1-x}Ge_x$ [3] and SiC [4] have been investigated and have been reported to have similar photoluminescent characteristics. The most widely accepted explanation for the origin of this phenomenon is the quantum confinement model [1,5], wherein the band gap of the material is widened by the presence of nanometric dots or wires formed on the porous surfaces by whatever process used to create them.

Porous films are usually made using anodization, stain etching, or a similar top-down method, but some attention has also been given to bottom-up methods such as low energy cluster beam deposition (LECBD). Random stacking of deposited clusters has been observed and ascertained to lead to porous films with materials of any kind (covalent and metallic) [6]. As for semiconductors, the photoluminescence of silicon nanocrystals has been investigated [7–10]; nanostructured silicon films have been obtained by neutral cluster depositions [11] and their optical properties have been investigated [12,13]. Numerical simulations have also been used to model the porosity of cluster-deposited films [14,15]. The simulations have shown that with a low enough deposition energy, clusters deposited with a cluster beam will not compress into epitaxial layers, but will instead form porous layers due to the resulting holes between the clusters [14]. Thus, it has

become clear that LECBD deposition can produce porous films very similar to etched films in terms of photoluminescent characteristics.

It has been shown that superimposed PS layers of differing porosities, also known as porous silicon multilayers, can be used to fabricate waveguide structures [16,17]. Multilayers such as these can be constructed by periodically varying the anodization parameters such as the current density [16]. When using LECBD, the same result should be attainable by periodically changing the deposition energy, although, to our knowledge, this has not previously been attempted. Furthermore, using a cluster beam to form the layers makes it possible to switch between different elements during the deposition process, thus resulting in multielemental multilayers and allowing further tailoring of optical properties.

The purpose of this study is to investigate the formation of porous semiconductor multilayers through cluster deposition. As a first step, the deposition of Ge clusters on a Si surface is simulated using molecular dynamics (MD). The porosity of the resulting layers is investigated as a function of deposition energy, and simulated transmission electron microscope (TEM) images of the layers are presented for comparison with experimental images. This work paves the way for the experimental deposition of porous Si and Ge multilayers.

2 Method

The LECBD of Ge clusters on Si was simulated using classical molecular dynamics. The atomic interactions were realized using Tersoff potentials for Si and Ge [18]. The temperature of the simulation cells was controlled at the

ᵃ e-mail: ari.harjunmaa@helsinki.fi

bottom 3 Å (corresponding to three atomic layers) of the substrates using the Berendsen temperature control algorithm [19] with a time constant of 250 fs. The bottom layer of atoms in each cell was fixed, to simulate the effect of a bulk substrate.

Prior to the deposition simulations, a cluster of 1018 Ge atoms (a suitable mean value for an experimental size distribution) was relaxed using multiple thermal annealing processes and then thermalized to 77 K, corresponding to the experimental setup of our laboratory, where the condensation chamber is cooled with liquid nitrogen. Likewise, a substrate of 27648 Si atoms (six unit cells thick) was relaxed and thermalized to 300 K to simulate a sample holder kept at room temperature. Then, using the parameters mentioned above, a single cluster was deposited on the substrate and observed for 10 ns to determine the behavior of the potential energy as a function of time, in an effort to find the minimum time step Δt between consecutive clusters that would allow sufficient relaxation of the deposited clusters. During the relaxation process, the potential energy showed very little change after deposition and none at all after 1 ns.

With this in mind, sets of up to 40 clusters were deposited at different energies ranging from 0.01 eV to 1.0 eV per atom, using a Δt value of 100 ps, or just enough time for a deposited cluster to reach the surface. The porosities of the resulting layers were calculated to determine the area of interest for the deposition energy. In the case of PS, it has been shown that the photoluminescence intensity of a layer is a function of the layer's porosity [5]. While the ideal porosity is above 70%, visible photoluminescence can still be detected from PS films with porosities well under 30% [20]. Thus, the goal in this study was to find the range of deposition energies that would result in porosities in the range of 30% to about 70%, which is close to the maximum porosity attainable with this method when depositing at thermal energies [13].

After this, the main simulations were initiated using the relevant deposition energies and a Δt of 1 ns. These simulations are currently running and will eventually serve to confirm and elaborate on the results obtained with the preliminary (low Δt) simulations presented here.

3 Results and discussion

3.1 Porosity

Porosity is defined as the proportion of the non-solid part of a layer volume to the total layer volume. In this work, the porosities P of the deposited layers were calculated according to the equation

$$P = 1 - \frac{Na_{\text{Ge}}^3}{N_0 V},\qquad(1)$$

where N is the total number of deposited atoms, a_{Ge} the lattice constant of germanium, N_0 the number of atoms in a Ge unit cell, and V the total volume of the deposited layer. The maximum porosity P_{max} was obtained using
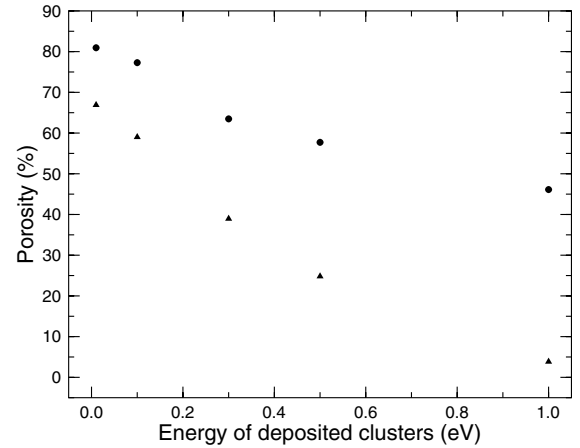
Fig. 1. Film porosities P_{max} (circle) and P_{min} (triangle) as a function of deposition energy per atom for runs of 30 deposited clusters.
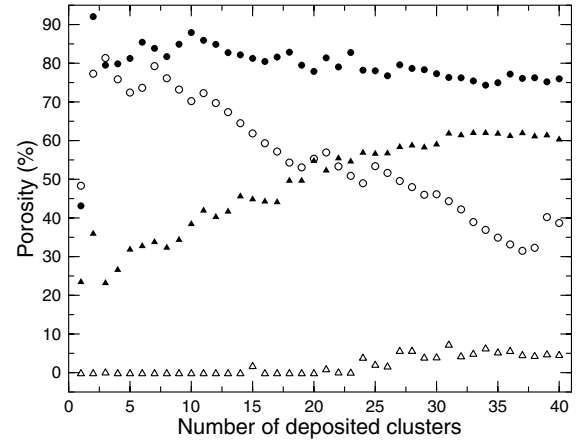
Fig. 2. Film porosities P_{max} (circle) and P_{min} (triangle) as a function of the number of deposited clusters for a deposition energy of 100 meV (filled) and 1 eV (open) per atom.

the maximum volume V_{max}, defined as the cuboid limited by the periodic boundaries of the cell and the height of the highest deposited atom; the minimum porosity P_{min} was obtained using the minimum volume V_{min}, where the volume was only integrated up to each surface atom [15]. The porosities thus calculated are presented as a function of deposition energy in Figure 1.

Both P_{max} and P_{min} clearly decrease as a function of the deposition energy, but although P_{min} eventually goes to zero, P_{max} seems to level off at around 50%. This is because there are too few deposited clusters — because of the way the porosities are calculated, surface roughness can cause a significant erroneous increase in P_{max} if the deposited layer is too thin. However, P_{min} is always too small for the opposite reason, since it does not take into account open crevices on the layer surface that may greatly contribute to a layer's actual porosity. It has been shown that as the volume-to-surface ratio η of a porous layer increases, the calculated porosities converge to a single value [15], as demonstrated in Figure 2. This means
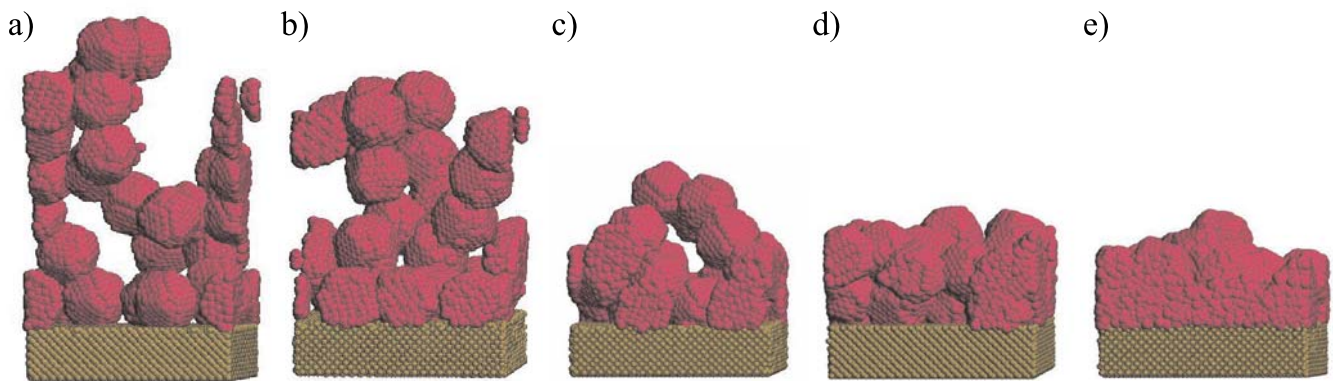
Fig. 3. Atomic cross-sections of deposited layers of 25 clusters with a deposition energy of (a) 10 meV, (b) 100 meV, (c) 300 meV, (d) 500 meV, and (e) 1 eV.
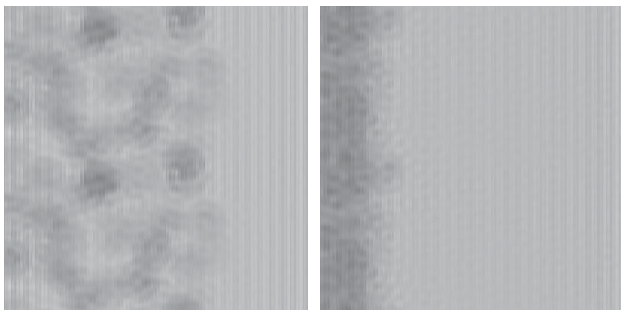
Fig. 4. Simulated cross-sectional TEM images of layers deposited using an energy of 10 meV (left) and 1 eV (right). The beam direction is from left to right.

that the more clusters are deposited, the closer P_{max} will be to the actual porosity — in reference [15], the number of clusters deposited ranged from 100 to 10^6.

When the deposition energy is increased to 1 eV per atom, it is clear from simple visual observation (as in Figure 3), and the fact that the porosities of Figures 1 and 2 drop to zero, that the layers are no longer porous. This is due to the compression and deformation of the energetic clusters upon impact. In this case, P_{max} is only an indication of the surface roughness, the effect of which is reduced as the volume of the deposited layer increases.

3.2 Image simulations

TEM image simulations of the deposited samples were performed using the program EMS [21]. The simulation parameters included a beam energy of 200 kV, an objective aperture of $2.0 \, \text{nm}^{-1}$, a spherical aberration of 1.0 mm and no defocus. The sampling was 1024×1024. The resulting images are presented in Figure 4.

In the 10 meV image, it is possible to distinguish columnar structures indicative of a porous layer [22]. In the 1 eV image, however, the deposited layer is nearly uniform with almost no distinctive features. This is due to the differences in atomic positions apparent in Figure 3: the

low-energy depositions leave different amounts of empty space within the layer, widening the image contrast, while the high-energy depositions produce a layer of uniform density, making the deposited clusters indistinguishable to the electron beam. Thus, it could be expected that an increase in porosity would result in an increase in image contrast in the deposited region.

4 Conclusion

The preliminary results indicate that the deposition energy range of interest for producing films with a porosity between 30% and 70% is about 10 meV to 500 meV per atom. Below 10 meV, not much increase in porosity can be expected, as the clusters do not compress at all and any variations are purely random; above 500 meV, the layers become completely compressed and no holes are formed between them. With further research, it will be possible to define empirical parameters for a fit function to describe layer porosity as a function of deposition energy. For this, the simulations must run for more than 40 clusters to ascertain that the calculated porosity values approach those of a layer of realistic thickness. Also, a longer Δt must be used to allow the deposited clusters to relax.

While the primary goal in using TEM image simulations is to be able to compare simulated images with experimental ones, the ultimate motivation is to find a quantitative way of measuring the porosity of the samples. Mapping image contrast as a function of layer porosity is one way to achieve this — another might involve using diffraction contrast imaging to find a method more sensible to slight differences in layer structure. Both methods can be simulated and thus combined with the MD simulations currently underway.

Keeping in mind several experimental limitations, we will attempt to construct similar porous layers experimentally. Instead of being able to use the monodisperse clusters with the well-defined deposition energies used in this study, the size distribution will be centered close to one thousand atoms using a quadrupole mass filter, and the

acceleration voltage will be tuned to find the appropriate porosity range. A disperse size distribution might have an additional effect on the relationship between deposition energy and layer porosity, an issue that remains to be investigated. TEM images of and photoluminescence measurements from the obtained samples will then serve to confirm the quality of the porous films.

References

1. L.T. Canham, Appl. Phys. Lett. **57**, 1046 (1990)
2. R. Venkatasubramanian, D.P. Malta, M.L. Timmons, J.A. Hutchby, Appl. Phys. Lett. **59**, 1603 (1991)
3. A. Ksendzov, R.W. Fathauer, T. George, W.T. Pike, R.P. Vasquez, A.P. Taylor, Appl. Phys. Lett. **63**, 200 (1993)
4. T. Matsumoto, J. Takahashi, T. Tamaki, T. Futagi, H. Mimura, Y. Kanemitsu, Appl. Phys. Lett. **64**, 226 (1994)
5. P.M. Fauchet, J. von Behren, Phys. Stat. Sol. B **204**, R7 (1997)
6. P. Mélinon, V. Paillard, V. Dupuis, A. Perez, P. Jensen, A. Hoareau, M. Broyer, J.L. Vialle, M. Pellarin, B. Baguenard, J. Lermé, Int. J. Mod. Phys. B **9**, 339 (1995)
7. J.R. Heath, Y. Liu, S.C. O'Brien, Q.-L. Zhang, R.F. Curl, F.K. Tittel, R.E. Smalley, J. Chem. Phys. **83**, 5520 (1985)
8. K. Fuke, K. Tsukamoto, F. Misaizu, M. Sanekata, J. Chem. Phys. **99**, 7807 (1993)
9. A.A. Seraphin, S.-T. Ngiam, K.D. Kolenbrander, J. Appl. Phys. **80**, 6429 (1996)
10. G. Ledoux, O. Guillois, D. Porterat, C. Reynaud, F. Huisken, B. Kohn, V. Paillard, Phys. Rev. B **62**, 15942 (2000)
11. P. Mélinon, P. Kéghélian, B. Prével, A. Perez, G. Guiraud, J. LeBrusq, J. Lermé, M. Pellarin, M. Broyer, J. Chem. Phys. **107**, 10278 (1997)
12. P. Mélinon, P. Kéghélian, B. Prével, V. Dupuis, A. Perez, B. Champagnon, Y. Guyot, M. Pellarin, J. Lermé, M. Broyer, J.L. Rousset, P. Delichère, J. Chem. Phys. **108**, 4607 (1998)
13. D. Amans, S. Callard, A. Gagnaire, J. Joseph, G. Ledoux, F. Huisken, J. Appl. Phys. **93**, 4173 (2003)
14. H. Haberland, Z. Insepov, M. Moseler, Phys. Rev. B **51**, 11061 (1995)
15. F. Voigt, R. Brüggemann, T. Unold, F. Huisken, G.H. Bauer, Mater. Sci. Eng. C **25**, 584 (2005)
16. M.G. Berger, C. Dieker, M. Thonissen, L. Vescan, H. Luth, H. Munder, W. Theiss, M. Wernke, P. Grosse, J. Phys. D **27**, 1333 (1994)
17. A. Loni, L.T. Canham, M.G. Berger, R. Arens-Fischer, H. Munder, H. Luth, H.F. Arrand, T.M. Benson, Thin Solid Films **276**, 143 (1996)
18. J. Tersoff, Phys Rev. B **39**, 5566 (1989)
19. H.J.C. Berendsen, J.P.M. Postma, W.F. van Gunsteren, A. DiNola, J.R. Haak, J. Chem. Phys. **81**, 3684 (1984)
20. K. Kordás, A.E. Pap, Sz. Beke, S. Leppävuori, Opt. Mater. **25**, 251 (2004)
21. P. Stadelmann, Ultramicroscopy **21**, 131 (1987)
22. A.G. Cullis, L.T. Canham, Nature **353**, 335 (1991)